· Article ·
doi: 10.13679/j.advps.2014.4.00261

Advances in Polar Science
December 2014 Vol. 25 No. 4: 261-268

Numerical simulation of the impact of underlying surface changes on Arctic climate

LIU Xiying* & XIA Huasheng

Institute of Atmospheric Physics, Chinese Academy of Sciences, Beijing 100029, China

Received 16 June 2014; accepted 15 September 2014

Abstract Using a regional atmospheric model for Arctic climate simulation, two groups of numerical experiments were carried out to study the influence of changes in the underlying surface (land surface, sea surface, and sea ice (LS/SS/SI)) from mild ice years to severe ice years on Arctic climate. In each experiment in the same group, the initial values and lateral boundary conditions were identical. The underlying surface conditions were updated every six hours. The model was integrated for 10 a and monthly mean results were saved for analysis. Variations in annual mean surface air temperature were closely correlated with changes in LS/SS/SI, with a maximum change of more than 15 K. The impact of changes in LS/SS/SI on low-level air temperature was also evident, with significant changes seen over the ocean. However, the maximum change was less than 2 K. For air temperature above 700 hPa, the impact of LS/SS/SI changes was not significant. The distribution of annual mean sea level pressure differences was coincident with the distribution of annual mean sea ice concentration. The difference centers were located in the Barents Sea, the Kara Sea, and the East Siberian Sea, with the maximum value exceeding 3 hPa. For geopotential height, some results passed and some failed a *t*-test. For results passing the *t*-test, the area of significance did not decrease with height. There was a significant difference at high levels, with a value of 27 gpm in the difference center at 200 hPa.

Keywords **land surface, sea ice, Arctic climate, numerical simulation**

Citation: Liu X Y, Xia H S. Numerical simulation of the impact of underlying surface changes on Arctic climate. Adv Polar Sci, 2014, 25: 261-268, doi:10.13679/j.advps.2014.1.00261

1 Introduction

The sun is the source of energy for atmospheric circulation. The surface of the Earth absorbs solar shortwave radiation and releases longwave radiation. The net amount of shortwave radiation within the atmosphere is regulated by terrestrial albedo, while the amount of longwave radiation is determined by the physical properties of the underlying surface of the Earth. Therefore, the underlying surface has an important role in determining and changing the Earth's climate. Changes in the physical properties of the Earth's surface affect the distribution of atmospheric energy and have a major impact on global climate.

The Arctic, a cold source in the Earth's climate system, has an important role in global energy balance. The Earth's rotation and uneven heating between the equator and the poles drive atmospheric circulation. Therefore, changes in the intensity of atmospheric heating in the polar regions significantly impact the atmospheric circulation[1], In recent decades, surface air temperatures in the Arctic have increased by almost twice the global average over the same period[2]. The term 'Arctic/Polar amplification effect' accurately describes the characteristics of climate change in the Arctic[3]. Because the Arctic region significantly impacts global climate patterns, increasing attention is being paid to the Arctic region and the role that it plays in the global climate system. The characteristics of climate change in the Arctic are reflected in the characteristics and patterns of climate change in the Northern Hemisphere and the Earth as a whole.

A prominent feature of the Arctic climate system is sea ice coverage. Sea ice is perennially frozen at the center of the Arctic, but it melts and refreezes seasonally at the periphery.

* Corresponding author (email: liuxy@lasg.iap.ac.cn)

Through dynamic effects, sea ice can be moved around. Sea ice has unique physical characteristics compared with seawater, and its existence has an important impact on the exchange of mass and energy between the atmosphere and the ocean. According to the Intergovernmental Panel on Climate Change (IPCC) report[4], satellite observations since 1978 have revealed an average reduction in Arctic sea ice coverage of 2.7% per decade, with the rate reaching 7.4% per decade for summer sea ice extent. Results from the European Centre for Medium-range Weather Forecasts (ECMWF) ERA-Interim reanalysis datasets have shown that the anticipated positive correlation between melting sea ice and rising temperatures has already occurred in the Arctic[5]. Over the past decade, the rapid melting of sea ice has strengthened that correlation.

Changes to the underlying surface in the Arctic region not only include changes in sea ice extent, sea surface temperature, and other ocean properties, but also quantitative changes in vegetation cover, leaf area index, and other land surface characteristics. Reanalysis datasets have contributed significantly to the understanding of the relationship between Arctic sea ice anomalies and atmospheric circulation, as well as the resultant impact on the climate in East Asia[6-7].

Although atmospheric models have been used for many years to study the impacts of sea ice on atmospheric circulation and the climate, these models have been based mainly on global dynamic framework[8]. In global numerical models that employ spherical coordinates, the North Pole is a singularity, for which velocity and direction cannot be defined. Further, with increasing proximity to the Pole, the time step required is reduced correspondingly. Conversely, regional models can address this issue and better describe the movements that pass through the North Pole. Furthermore, regional models can be used to obtain higher resolution results. However, to date, regional models have not been widely used to investigate the Arctic climate.

The aim of this study was to use regional numerical simulations to investigate the impact of changes in the underlying surface (land surface, sea surface, and sea ice (LS/SS/SI)) on the Arctic atmosphere. Two groups of values were tested. The first compared a typical mild sea ice year with the lower boundary conditions changed to those of a severe sea ice year. The second compared a typical severe sea ice year with the lower boundary conditions changed to those of a mild sea ice year. With this approach, we hoped to improve the understanding of the effect of the underlying surface on the Arctic climate.

2 Design of the numerical experiments

In this paper, we used the Weather Research and Forecasting (WRF) model with a polar climate extension (WRF/PCE)[9]. The model was used to perform numerical experiments to study the impact of changes in LS/SS/SI on the Arctic climate. The configuration of model parameters was determined by the results of combination experiments involving parameterization schemes of different physical processes. This was to ensure suitability of the model for simulating the regional Arctic climate. The regional center of the simulation was the North Pole. The model had a horizontal resolution of 50 km, with a time step of 180 s. In all integrations, there were a total of 84 × 96 horizontal grid points, and the model was divided into 27 vertical layers. The following schemes were used for the parameterization of physical processes: the WRF Single-Moment 3-class Microphysics (WSM3) scheme for ice; Monin–Obukhov surface layer scaling; the Yonsei University (YSU) planetary boundary layer scheme; the Dudhia shortwave radiation scheme; the Rapid Radiative Transfer Model (RRTM) longwave radiation scheme; and the Pleim–Xiu land surface model.

Given that sea ice forms a significant portion of the underlying surface of the Arctic, typical severe and mild sea ice years were used to select low boundary conditions for investigating the impact of surface changes on Arctic climate. Sea ice concentration from the ECMWF ERA-Interim datasets (1.5° × 1.5°) was used to compute the annual mean sea ice coverage in the simulation domain from 1989 to 2008 (Figure 1). From the results, the years 1998 and 2007 were selected as typical severe and mild sea ice years, respectively. Because these were not years with historically extreme values of sea ice extent, the simulation results are of general significance. The underlying surface physical conditions for the two years were then used as low boundary conditions to drive the model to study the impact of surface changes on the Arctic climate. The physical variables for the low boundary conditions were sea ice extent, sea surface temperature, vegetation cover, leaf area index, and terrestrial albedo.

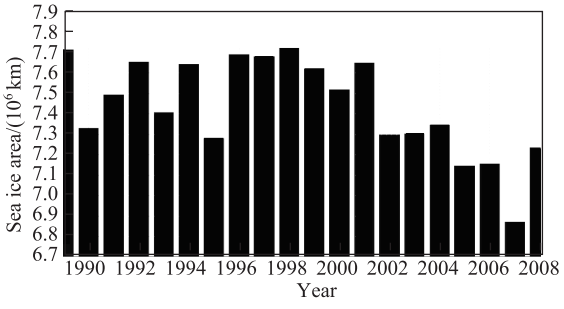

Figure 1 Annual mean sea ice coverage from 1989 to 2008 in the ERA-Interim reanalysis dataset.

Numerical simulations using the WRF/PCE model were carried out under the following conditions (Table 1): (i) year 2007 (hereafter referred to as S2007); (ii) year 1998 (S1998); (iii) year 2007 with the underlying surface conditions of 1998 (S2007_1998L); and (iv) year 1998 with the underlying surface conditions of 2007 (S1998_2007L).

The experiments were divided into two groups: (a) S2007 and S2007_1998L and (b) S1998 and S1998_2007L. The experiments within each group shared the same initial

Table 1 Design of the numerical experiments

Experiment name		Integration time/a	Initial field	Lower boundary	Lateral boundary
Group a	S2007	10	2007	2007	2007
	S2007_1998L	10	2007	1998	2007
Group b	S1998	10	1998	1998	1998
	S1998_2007L	10	1998	2007	1998

value and lateral boundaries. The 1.5° × 1.5° ERA-Interim reanalysis dataset was used for modeling, and both sets of boundary conditions (lower and lateral) were updated every six hours, resetting to the start of the year when the current year ended. The integration time for all experiments was 10 a. The mean monthly results were exported, and the 10-year means were used to analyze the impact of surface conditions on the climate. Although the simulation results could be used to analyze the impact of the lateral boundary conditions (e.g., by comparing the difference between S2007 and S1998_2007L), this was outside the scope of the present study.

3 Analysis of simulation results

Two sets of simulation results were obtained from the experiments. For Group (a), comprising S2007 and S2007_1998L, the underlying surface conditions were changed from a mild to a severe sea ice year. For Group (b), comprising S1998 and S1998_2007L, the underlying surface conditions were changed from a severe to a mild sea ice year. To confirm the reliability of the results, the changes were subjected to a Student's *t*-test, with a significance level of α=0.05. Analyses of the changes in temperature, sea level pressure, and geopotential height are presented below.

3.1 Temperature

Changes in surface air temperature for Group (a) are shown in Figure 2a. During times of severe sea ice, the temperature over most of the domain decreased. Figure 2a shows two regions with significant temperature variations, the East Siberian and Laptev Seas, where the core difference was more than 6 K, and the Barents and Kara Seas, with an even larger core difference of 15 K. There were temperature increases in the Beaufort Sea and in some coastal areas of southern Greenland, which corresponded to a reduction in sea ice in those locations.

Changes in surface air temperature for Group (b) are shown in Figure 2b. There was a significant increase in surface air temperature during mild sea ice years. Areas with significant temperature variations included the East Siberian and Laptev Seas (with a core difference of more than 6 K) and the Barents and Kara Seas (with a core difference of more than 18 K). The temperature decreased over the Beaufort Sea and in some coastal areas of southern Greenland, which corresponded to an increase in sea ice in those locations.

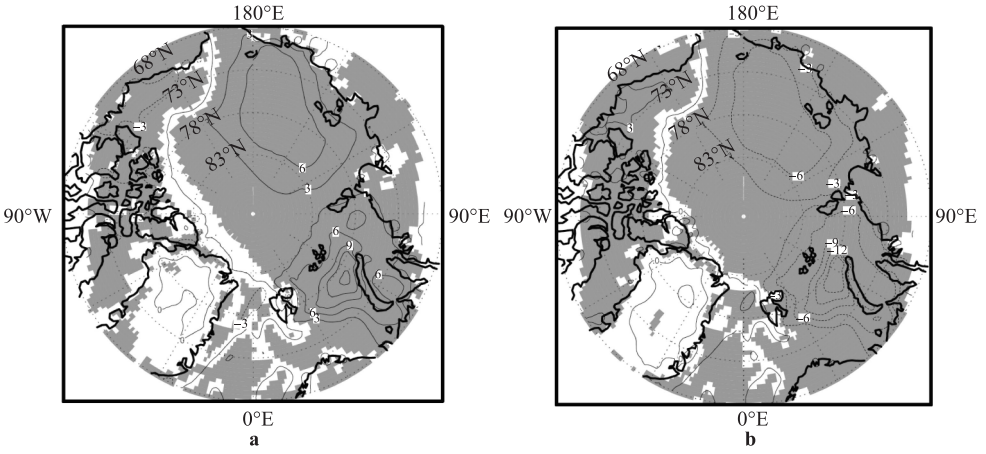

Figure 2 Differences in the 10-year mean air temperature at 2 m for Group a (**a**) and b (**b**). Contour interval is 3 ℃. Shaded areas: Passed *t*-test, α=0.05.

For both groups, the surface air temperature distributions exhibited similar patterns, but with the signs reversed, reflecting the different underlying surface conditions for the two sets of experiments. Essentially, an increase in the amount of sea ice corresponded to a downward sensible heat flux and a positive anomaly in latent heat flux, and vice versa. Therefore, the results of the numerical simulations fit within theoretical limits. Interestingly, the symbols for the deviation in both downward longwave and shortwave radiation fluxes over the Norwegian Sea and Nordic land areas for the two experimental groups were opposite. This is possibly a result of differences in polar medium level clouds. The resulting difference between S2007 and S1998 was similar to Figure 2a, indicating that surface temperature was mainly affected by the underlying surface.

Changes in air temperature at 850 hPa are shown in

Figure 3. Although the areas with significant temperature differences (shaded in gray) are fairly similar between the two groups, the degree of similarity is less than that for surface air temperatures (Figure 2). The areas with significant regional differences are also reduced. While the signs are reversed between the two groups, as was the case with surface air temperatures in Figure 2, the absolute deviations in Figure 3 are smaller than in Figure 2.

There are two positive centers of temperature difference at 850 hPa between S2007 and S1998, one close to Siberia, and the other close to Russia and the European continent (figure not shown). Both centers correspond to the positive center of the surface temperature difference (Figure 2a). This difference from the patterns seen in Figure 3a reflects the impact of lateral boundary conditions.

At 500 hPa, the impact of changes to the underlying surface was further reduced. For Group (a), only one area with a positive value over the Arctic Ocean passed the significance test, with a value of 0.5 K; For Group (b), there was also only one area with a positive value near the Barents Sea that passed the significance test, with a value of approximately 0.18 K (figures not shown). At a height of 200 hPa, there were no significant differences (figures also not shown).

The analysis presented above showed that changes in the underlying surface had an impact on surface air temperature, with the largest difference being more than 15 K. However, with increasing height, other atmospheric processes (for example, internal atmospheric variability) may play a more significant role in affecting temperature change and the impact of the underlying surface on atmospheric temperature decreases correspondingly. In the middle and upper levels of the atmosphere, changes in the underlying surface no longer have any significant impact.

The annual variations in regionally averaged temperatures caused by changes in the underlying surface are shown in Figure 4. For both groups, significant differences are seen mainly below 500 hPa, consistent with the results presented above. However, significant differences exist between the two groups at heights well above the surface (for example, for Group (a), significant difference occurred

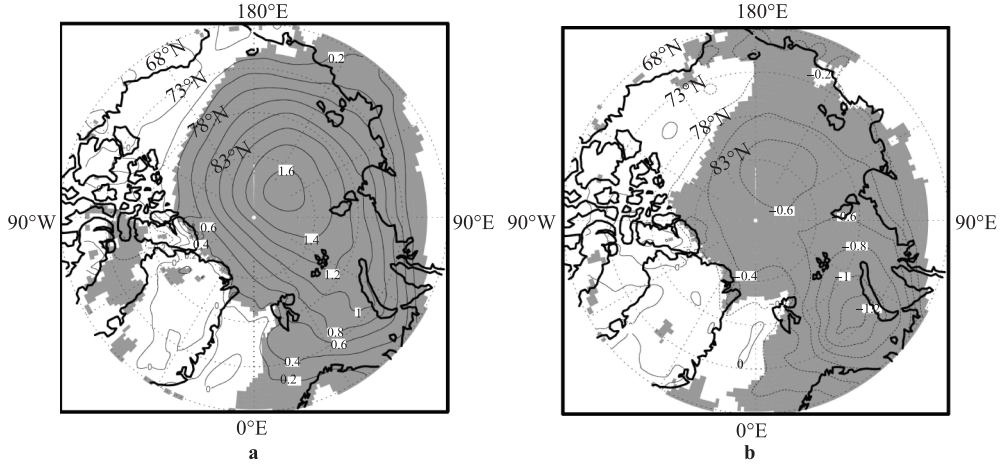

Figure 3 Differences in the 10-year mean air temperature at 850 hPa for Group a (**a**) and b (**b**). Contour interval is 0.2 ℃. Shaded areas: Passed *t*-test, α=0.05,

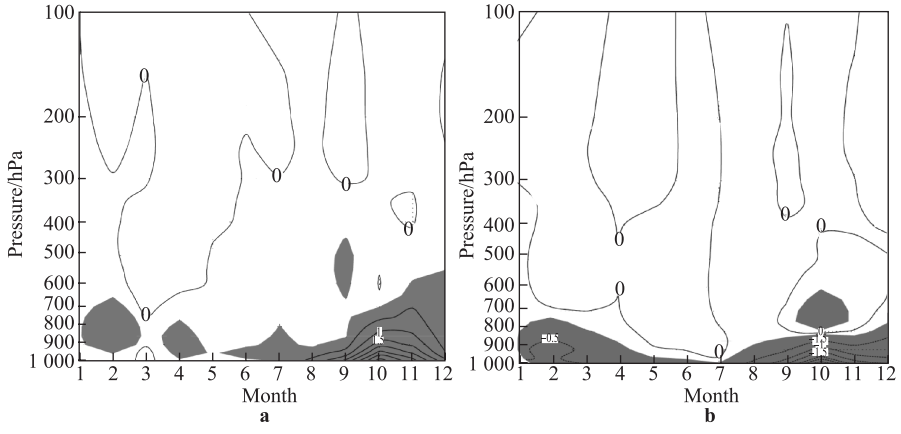

Figure 4 Distributions of 10-year regionally averaged air temperature differences Group a (**a**) and b (**b**). Contour interval is 0.2℃. Shaded areas: Passed *t*-test, α=0.05.

in September at 550 hPa, while for Group (b), a significant difference occurred in October at 700 hPa), which may be a result of other physical processes that impact temperature. However, further studies are required to determine the specific mechanism(s).

For both groups, the atmospheric height that showed significant difference is higher in February and October–December, but there is little difference for January. For Group (a), the March and May temperature differences were not significant. However, for Group (b), regions with significant temperature differences in March reached 800 hPa. The May temperature difference at 1 000 hPa was also significant.

3.2 Sea level pressure

The spatial distribution of annual mean sea level pressure differences is shown in Figure 5. In severe sea ice year conditions, there was a significant increase in pressure over the Barents, Kara, and East Siberian Seas (Figure 5a). During a mild sea ice year, the pressure over these regions decreased significantly (Figure 5b). From this, the pressure changes appeared to be related to the sea ice concentration, secondary to the thermal forcing effect of the surface.

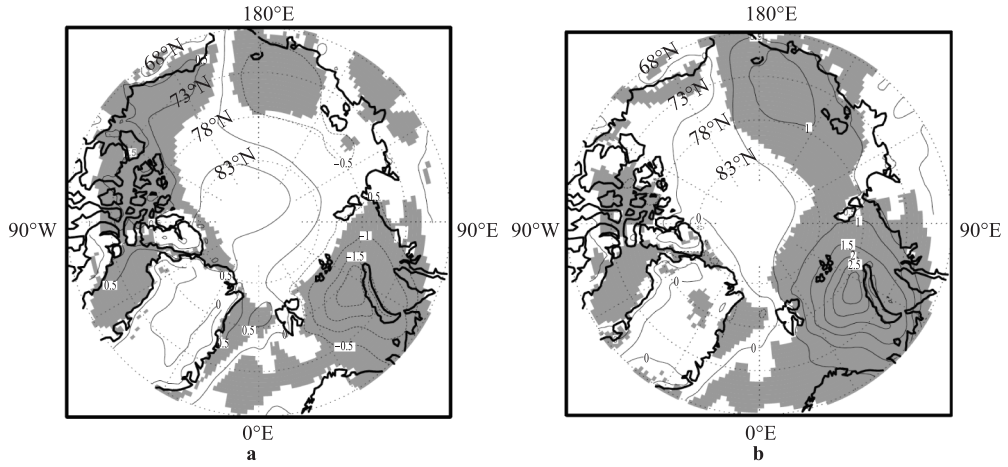

Figure 5 Differences in the 10-year mean sea level pressure for Group a (**a**) and b (**b**). Contour interval is 0.5 hPa. Shaded areas: Passed *t*-test, α=0.05.

The change in sea level pressure was greater for Group (b), and the absolute value of both differential centers were around 0.5 hPa higher than for Group (a). Group (a) showed a significant difference in sea level pressure over northern Greenland, the Canadian Arctic Archipelago, and the northern waters of North America. However, there was no such difference for Group (b).

3.3 Geopotential height

The impacts of changes to the underlying surface on geopotential height at the 850 and 500 hPa isobaric surfaces are shown in Figures 6 and 7. For both isobaric surfaces, the major characteristic of the differences in geopotential height was that the cooling and warming effects in the underlying surface forced a corresponding reduction (Figures 6a and 6b) and increase (Figures 7a and 7b) in geopotential height, respectively. Further, the two differential centers in geopotential height were both close to the North Pole, causing a strengthening and weakening of the polar vortex intensity, in response to cooling and warming, respectively.

It is conspicuous that the major changes in geopotential height were responses to the thermal forcing changes in the underlying surface. The difference is that for Group (a), the maximum absolute value of the differential centers in geopotential height for 850 and 500 hPa was larger than 16 and 27 gpm, respectively. For Group (b), the values were much smaller and the entire simulation domain did not pass the significance test for difference in geopotential height (Figures 6b and 7b). It should also be noted that for Group (a), the region with a significant difference in geopotential height was larger at 500 hPa (Figures 6a and 7a).

The pattern of change in geopotential height at 200 hPa (figures not shown) was similar to those in the middle and upper layers of the atmosphere. For Group (a), areas with a significant difference existed, with the largest value in differential center being greater than 27 gpm. There was no significant difference in geopotential height for Group (b).

The annual variation in regionally averaged geopotential height is shown in Figure 8. The two groups were markedly different. For Group (b), there was a significant difference in geopotential height at 600–300 hPa in May, but no difference at any level for the other months (Figure 8b). However, for Group (a), there were distinct characteristics for each month. There was no significant impact from January to June, or for August, but significant impacts were noted in July (at 800–250 hPa) and from September to December (at 850–200 hPa) (Figure 8a).

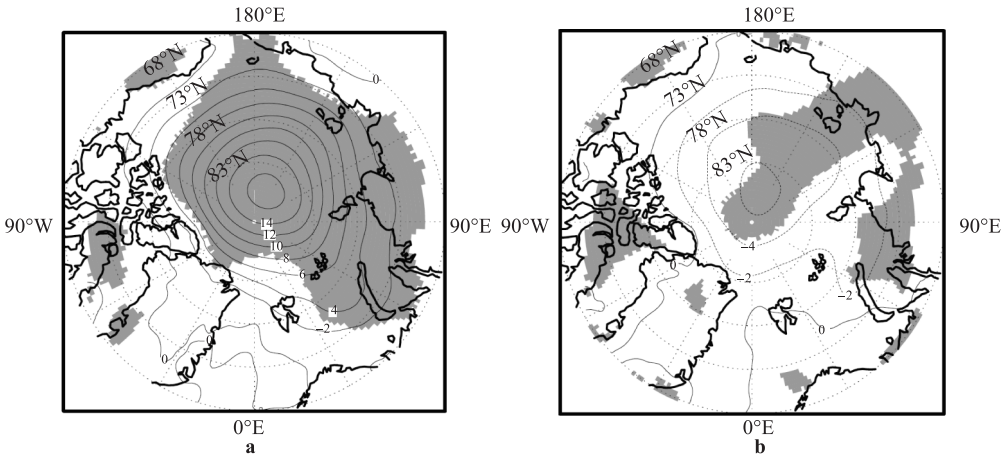

Figure 6 Differences in the 10-year mean geopotential height at 850 hPa for Group a (**a**) and b (**b**). Contour interval is 2 gpm. Shaded areas: Passed *t*-test, α=0.05.

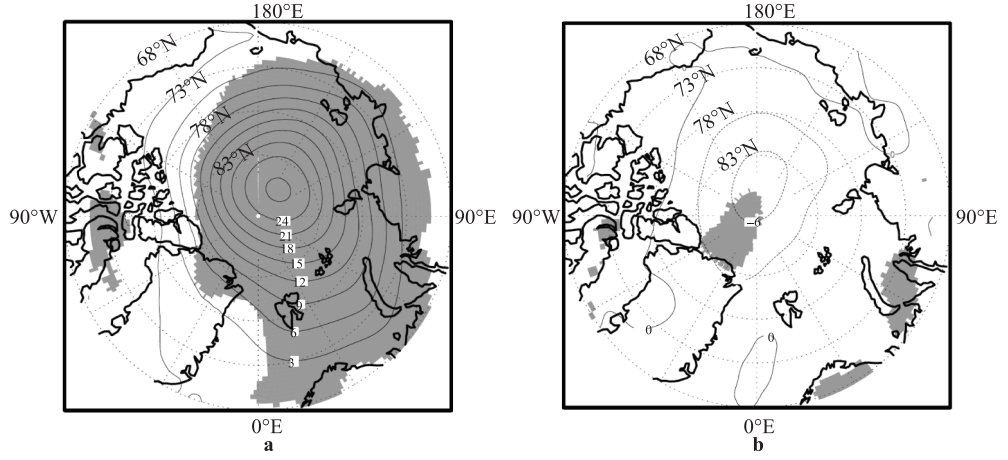

Figure 7 Differences in the 10-year mean geopotential height at 500 hPa Group a (**a**) and b (**b**). Contour interval is 3 gpm. Shaded areas: Passed *t*-test, α=0.05.

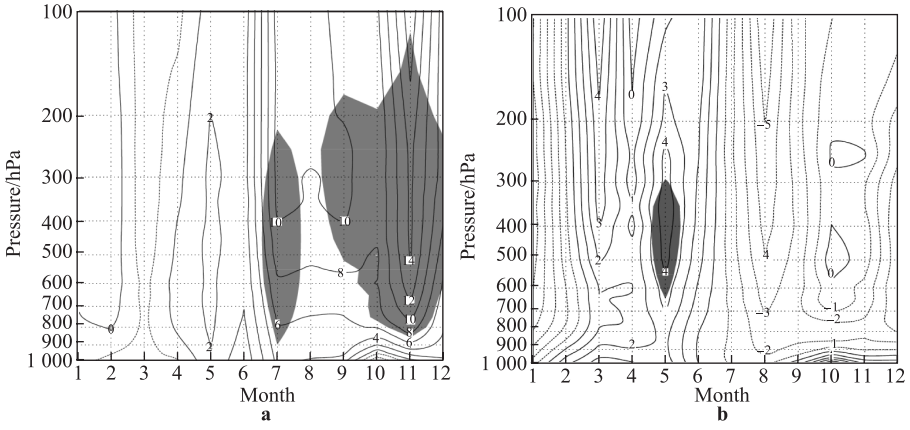

Figure 8 Distributions of 10-year regionally averaged geopotential height for Group a (**a**) and b (**b**). Contour interval is 3 gpm. Shaded areas: Passed *t*-test, α=0.05.

The above analysis shows that the significant difference in geopotential height is not necessarily inversely related to atmospheric height. Under certain scenarios, the changes in the underlying surface had a significant impact on the geopotential height, even in the upper atmosphere.

4 Summary and discussions

To study the impact of changes in the underlying surface on Arctic climate, the regional climate model WRF/PCE, which was based on and developed from the WRF model, was used to conduct numerical simulations. Two groups of values were tested. The first compared a typical mild sea ice year (2007) with the lower boundary conditions changed to those of a severe sea ice year (1998). The other compared a typical severe sea ice year (1998) with the lower boundary conditions changed to those of a mild sea ice year (2007).

During the experiments, the lower boundary conditions were changed every six hours. These included sea ice extent, sea surface temperature, vegetation cover, leaf area index, and terrestrial albedo. The soil and ground temperatures were separately calculated using the land surface process model. By analyzing the differences between the control and manipulated experiments for each group, we determined the impact of changes to the underlying surface on Arctic climate. The major conclusions are as follows:

The impact of changes in the underlying surface on atmospheric temperatures was significant, and the largest difference was greater than 15 K. For the two groups, changes in the underlying surface conditions led to results with opposite signs, indicating the direct forcing of a cold versus heat source. Temperature changes also exhibited the typical characteristics of a thermal response, and as atmospheric height increased, the impact of the underlying surface on temperature decreased. The impact became insignificant in the middle and upper atmospheric levels.

Regions with significant changes in sea level pressure included the Barents, Kara, and East Siberian Seas, with the largest difference being greater than 3 hPa. The pattern corresponded with that of mean annual sea ice concentration.

Thermal forcing of the underlying surface caused a difference in the geopotential height at both 850 and 500 hPa. The two centers with significant differences in geopotential height were near the North Pole, and resulted in changes in polar vortex strength. However, the significant difference in geopotential height was markedly distinct between the two groups. In addition, the difference did not necessarily decrease with increase in atmospheric height. Under certain scenarios, the changes in the underlying surface had an impact on geopotential height even in the upper atmosphere.

This study mainly compared the differences between two experimental groups, while holding the initial value and lateral boundary conditions of the model constant. We did not analyze the impact of the lateral boundary conditions (i.e., the external atmosphere). Although the impact of surface changes in the two groups was exactly opposite, there was no parallel in the atmospheric response, with a relatively large significant difference. This indicated that the impact of other physical processes, especially those involving interactions between the land and atmosphere, might have played a greater role.

The present work is typical of similar research using forcing-response approximation. The relationship between the circulation anomalies in the Arctic atmosphere and changes in the underlying surface (e.g., sea ice) was studied through data analyses and the relationships that were determined were purely statistical. The results did not directly approximate physical processes, although the statistical explanation is a type of approximation (filtering). The Arctic climate was simulated on an annual basis, and the process did not involve a longer time frame. Therefore, the findings cannot be compared with those obtained by studies that made use of reanalysis data, for example, Wu et al. [7]. There is a relative lack of research on the Arctic climate using regional models for simulation, and this study was just an initial step. In-depth inspection and evaluation of the model performance should be conducted.

The Arctic region is an area with strong interactions between the sea ice and the atmosphere. The Arctic climate is a result of the combined action of physical processes occurring at the Earth's surface and in multiple atmospheric levels above. In this study, the lower boundary conditions were set and the atmospheric mode was used for the integration experiments. The results indicated atmospheric responses to external forces. However, it is known that the long-term average state of the atmosphere (in the traditional climatic sense) is the result of complex interactions within the atmosphere itself, as well as with land, sea, and sea ice, and these components are in continuous flux. Although it has its own complications[10], using a coupled system model in future research may result in a more accurate simulation of the Arctic climate.

Acknowledgments The work was sponsored by the Natural Science Foundation of China (Grant no. 41276190). The ERA-Interim reanalysis datasets were downloaded from the ECMWF data server website. The Student's *t*-tests were calculated using the clim.pact package in R.

References

1 Serreze M C, Barry R G. The Arctic climate system. Cambridge: Cambridge University Press, 2005: 56–60.
2 IPCC. Fourth Assessment Report: Climate Change 2007: The AR4 Synthesis Report. Geneva: IPCC, 2007: 30–31.
3 Serreze M C. Francis J A. The Arctic amplification debate. Climate Change, 2006, 76(3-4): 241–264.
4 Solomon S, Qin D, Marquis M, et al. Climate Change 2007: The Physical Science Basis. Cambridge: Cambridge University Press, 2007: 5–6.
5 Screen J A, Simmonds I. The central role of diminishing sea ice in recent Arctic temperature amplification. Nature, 2010, 464(7293): 1334–1337.
6 Wu B Y, Wang J, Walsh J E. Dipole anomaly in the winter Arctic atmosphere and its association with sea ice motion. Journal of

Climate, 2006, 19(2): 210–225.

7 Wu B Y, Zhang R H, Wang B. On the association between spring Arctic sea ice concentration and Chinese summer rainfall: A further study. Advances in Atmospheric Sciences , 2009, 26(4): 666–678.

8 Huang S S, Yang X Q, Xie Q. Observation data analysis and numerical simulation of influences of Arctic sea ice on atmospheric general circulation and climate. Acta Oceanologica Sinica, 1992, 14: 30–46.

9 Liu X Y, Zhao J H, Xia H S, et al. Temperature biases in modeled polar climate and adoption of physical parameterization schemes. Advances in Polar Science, 2013, 23(1): 30–40.

10 Liu X Y. Biases of the Arctic climate in a regional ocean–sea ice atmosphere coupled model: an annual validation. Acta Oceanologica Sinica, 2014, 33(9): 56–67.